Traffic signal coordination control for arterials with dedicated CAV lanes

Liang Xu
Department of Beihang Hangzhou Innovation Institute Yuhang, Hangzhou, China
Sheng Jin and Bolin Li
College of Civil Engineering and Architecture, Zhejiang University, Hangzhou, China and
Department of Alibaba-Zhejiang University Joint Research Institute of Frontier Technologies, Hangzhou, China, and
Jiaming Wu
Department of Architecture and Civil Engineering, Chalmers University of Technology, Gothenburg, Sweden

Abstract

Purpose – This study aims to make full use of the advantages of connected and autonomous vehicles (CAVs) and dedicated CAV lanes to ensure all CAVs can pass intersections without stopping.

Design/methodology/approach – The authors developed a signal coordination model for arteries with dedicated CAV lanes by using mixed integer linear programming. CAV non-stop constraints are proposed to adapt to the characteristics of CAVs. As it is a continuous problem, various situations that CAVs arrive at intersections are analyzed. The rules are discovered to simplify the problem by discretization method.

Findings – A case study is conducted via SUMO traffic simulation program. The results show that the efficiency of CAVs can be improved significantly both in high-volume scenario and medium-volume scenario with the plan optimized by the model proposed in this paper. At the same time, the progression efficiency of regular vehicles is not affected significantly. It is indicated that full-scale benefits of dedicated CAV lanes can only be achieved with signal coordination plans considering CAV characteristics.

Originality/value – To the best of the authors' knowledge, this is the first research that develops a signal coordination model for arteries with dedicated CAV lanes.

Keywords Connected and automated vehicles, Dedicated lane, Arterial signal coordination

Paper type Research paper

1. Introduction

With the rapid development of automotive technology, connected and autonomous vehicles (CAVs) have been widespread concerned and become one of the focuses in view of researchers on automotive engineering and traffic engineering. CAVs admittedly have remarkable advantages over regular vehicles (RVs) in many aspects. Firstly, CAVs are connected with the surrounding vehicles and roadside infrastructures and can communicate with them to exchange real-time traffic information, such as vehicle status, traffic signal status and intersection geometry. Secondly, CAVs can perform driving functions (e.g. steering, acceleration and braking) all by themselves and have shorter reaction time than human drivers. Thus, CAVs can not only provide a new source of data for traffic management but also can be treated as actuators in traffic flow (Yang *et al.*, 2021). These features of CAVs provide a solid foundation to improve traffic operations in transportation systems (Peng *et al.*, 2021; Larsson *et al.*, 2021).

In the past few years, different methods have been developed to use CAV advantages to promote traffic signal control performance. One concept is to treat CAVs as motion detectors to supersede traditional traffic detectors. Traditional detectors are fixed in position. The obtained information is inaccurate and limited spatially. With the advent of CAVs, the data is renovated. And real-time, accurate and high-resolution traffic data can be provided for traffic signal control. Based on the information of CAV positions, headings and speeds, predictions on traffic flow state are made to optimally allocate green time to serve traffic from different approaches to achieve

This study was supported by "Pioneer" and "Leading Goose" R&D Program of Zhejiang (2022C01042), and Alibaba-Zhejiang University Joint Research Institute of Frontier Technologies.

Received 31 August 2021
Revised 11 January 2022
9 February 2022
11 February 2022
Accepted 22 February 2022

The current issue and full text archive of this journal is available on Emerald Insight at: **https://www.emerald.com/insight/2399-9802.htm**

Journal of Intelligent and Connected Vehicles
5/2 (2022) 72–87
Emerald Publishing Limited [ISSN 2399-9802]
[DOI 10.1108/JICV-08-2021-0015]

the best system performance. These approaches are applied to isolated intersection (Goodall *et al.*, 2013), artery (Beak *et al.*, 2017) and transit system (Zeng *et al.*, 2015). The methods above only use CAV data to grasp the traffic state. The movements of CAVs are not optimized to improve mobility. Then, researchers put forward a new idea to integrate signal optimization and CAV trajectory planning. For intersections, the optimization framework usually consists of two levels. Phase sequences, green start and duration of each phase, and cycle lengths are optimized to minimize the intersection delays and number of stops. In terms of CAVs, trajectories are optimized to minimize fuel consumption/emission. These two tasks are optimized jointly (Du *et al.*, 2021; Fayazi and Vahidi, 2018; Feng *et al.*, 2018; Guo *et al.*, 2019a, 2019b; Li *et al.*, 2014; Xu *et al.*, 2018). Also, the optimization range is extended to arteries (He *et al.*, 2015; Yang *et al.*, 2021; Qian *et al.*, 2021). Besides signal timing plan at intersections, Yang *et al.* (2021) optimized the offsets for every cycle. CAVs are controlled to form compact platoons by cooperative adaptive cruise control. Aggregating vehicles into platoons could reduce the computation burden, making it more practical to be implemented in the real world. He *et al.* (2015) took queues at intersections into consideration to avoid suboptimal or infeasible solutions to optimal vehicle trajectory on signalized arteries.

Great achievements have been made in the area of CAV-based traffic management, but there are still several limitations. Most of the studies are conducted under a 100% CAV environment or a mixed traffic environment with high penetration rate of CAVs. Although it is expected that the penetration rate of CAVs may dramatically increase in the future, there is still a long way to achieve such a goal of high CAVs penetration or fully automated vehicles (Guo *et al.*, 2019a, 2019b). The benefit on traffic operation, including reduced traffic congestion, increased safety, energy conservation and pollution reductions, will only be significant when CAVs become common and affordable, probably in the 2050s to 2060s (Litman, 2017). In other words, CAVs will be traveling along urban roads with RVs at a relatively low penetration rate for quite a long time.

Be aware of this point, researchers analyzed the characteristics of mixed traffic flow under different penetration rates. Chang *et al.* (2020) analyzed the traffic stability for mixed traffic flow. It is found that if the speed is higher than the critical speed, the stability of the mixed traffic flow decreases with the increase of the penetration rate. Ghiasi *et al.* (2017) declared that CAVs should not be taken as a sure means of increasing road capacity. The actual headway settings (Ghiasi *et al.*, 2017), reaction time settings (Hu *et al.*, 2021) and the CAVs platoon length (Sala and Soriguera, 2021) will all affect the capacity. Some settings even lead to decreases in capacity with CAV penetration rate. People's perception on AV safety is critical to the pace and success of deploying the AV technology (Shi *et al.*, 2021). However, the safety benefits of CAVs are not proportional to CAV penetration (Sinha *et al.*, 2021). At low levels of CAV penetration rate, the safety improvements were found to be marginal (Arvin *et al.*, 2021). Full-scale benefits of CAVs can only be achieved at 100% CAV penetration. From a strategical planning perspective, dedicated lanes are preferable to attain the positive effects of CAVs (Carrone *et al.*, 2021). Predictably, dedicated CAV lanes will be an important segment in CAV implementation.

In past decades, many strategies were proposed to optimize arterial signal to improve the traffic efficiency. Little *et al.* (1981) first proposed the MAXBAND model in the form of a mixed-integer linear program to optimize arterial signal. Then, with consideration of different traffic flow patterns, Gartner *et al.* (1991) developed MULTIBAND model to generate a variable bandwidth progression. Based on these two models, AM-BAND (Zhang *et al.*, 2015), MaxBandLA (Zhang *et al.*, 2016), OD-BAND (Arsava *et al.*, 2016) and PM-BAND (Ma *et al.*, 2018) were developed to adapt to various scenarios. However, there is little research on arterial signal coordination with dedicated CAV lanes at low CAV penetration. In this research, we propose a new signal coordination method to promote efficiency of arteries with dedicated CAV lanes. This method can be used for signal optimization alone, and can also be applied as the basis for trajectory optimization of CAVs.

The paper is organized as follows. In Section 2, the model formulation is described. Section 3 presents a case study with different CAV flowrate. Section 4 gives sensitivity analysis. Section 5 concludes the paper.

2. Methodology

2.1 Problem description

Arterial coordination for RVs is to synchronize signal timing plans between intersections to produce a progression band along the arteries as wide as possible. As vehicles are from different directions and have various routes, a wider band allows vehicles to have more opportunity to pass through artery without stopping. CAVs have a communication function and can act as actuators. They can obtain traffic signal status in advance. And their trajectories can be planned according to traffic signal status and traffic state. Meanwhile, the flowrate of CAV will not exceed the dedicated lane capacity. Thus, we only need to ensure that CAVs entering during the green light have the track to pass the downstream intersection without stopping within a certain speed range.

2.2 Modeling assumptions

Before developing the model, some assumptions are proposed to simplify the problem, which are listed as follows:

- The dedicated CAV lane is continuous along the arterial road.
- Regular lanes can be borrowed to adjust the passing order within CAVs.
- In most time, CAVs will pass within the dedicated lane. Thus, CAVs can be separated from RVs, and will not affect the operation of RVs significantly.

2.3 Model development

In the model, we assume that CAVs can obtain the exact distance between intersections and signal timing plans of intersections in real time. To ensure the mobility and safety of CAVs, the average speed of CAVs between intersections is limited within a range. The modeling process is shown as follows. The notations needed in formulation are defined in Table 1. Most of the time variables are in units of cycle time to linearize the model.

Table 1 Notations of model parameters and variables

Notation	Description
$b_i(\bar{b}_i)$	The outbound (inbound) bandwidth for link i (cycles)
$w_i(\bar{w}_i)$	The part of a green duration before (after) the green band in outbound (inbound) direction (cycles)
$\tau_i(\bar{\tau}_i)$	The queue clearance time (cycles)
θ_i	The offset of intersection i (cycles)
$n_i(\bar{n}_i)$	Integer variables to represent the number of signal cycles
$r_{s\_out,i}(\bar{r}_{s\_out,i})$	The total red duration at the left(right) side of outbound straight-moving phase at intersection i (cycles)
$r_{l\_out,i}(\bar{r}_{l\_out,i})$	The total red duration at the left(right) side of outbound left-turning phase at intersection i (cycles)
$r_{s\_in,i}(\bar{r}_{s\_in,i})$	The total red duration at the left(right) side of inbound straight-moving phase at intersection i (cycles)
$r_{l\_in,i}(\bar{r}_{l\_in,i})$	The total red duration at the left(right) side of inbound left-turning phase at intersection i (cycles)
$g_{s\_out,i}$	The green duration of outbound straight-moving phase at intersection i (cycles)
$g_{s\_in,i}$	The green duration of inbound straight-moving phase at intersection i (cycles)
$g_{l\_out,i}$	The green duration of outbound left-turning phase at intersection i (cycles)
$g_{l\_in,i}$	The green duration of inbound left-turning phase at intersection i (cycles)
$\delta_i(\bar{\delta}_i)$	Binary decision variable that represents the phase sequences at intersection i
$d_i(\bar{d}_i)$	Distance of link i in outbound(inbound) direction
v_{max}	The limited maximum average velocity of CAVs
v_{min}	The limited minimum average velocity of CAVs
$t_{max,i}(\bar{t}_{max,i})$	The maximum travel time for CAVs on link i in outbound(inbound) direction
$t_{min,i}(\bar{t}_{min,i})$	The minimum travel time for CAVs on link i in outbound(inbound) direction
$\lambda_i(\bar{\lambda}_i)$	The difference between maximum and minimum travel time on link i in outbound(inbound) direction

2.3.1 Signal phase sequence

National Electrical Manufacturers Association (NEMA) phase designation, in accordance with NEMA TS-1 standards, is applied in the model. As shown in Figure 1, conflicting flows in opposite directions lie on the same ring. And a barrier is set between flows from different roads. The phase sequence on the same ring can be interchangeable without crossing the barrier. As only flows on the arteries are considered in the model, the sequence of phase in the red dotted frame will be optimized.

A set of binary integer variables $\delta_i(\bar{\delta}_i)$ is defined to represent sequences of two phases within the same cycle. If the outbound (inbound) straight-moving phase lies before the inbound (outbound) left-turning phase, $\delta_i(\bar{\delta}_i)$ is equal to one. Otherwise, $\delta_i(\bar{\delta}_i)$ is equal to zero.

Then, the red duration before/after different phases can be determined according to equations (1)–(8).

$$r_{s\_out,i} = (1-\delta_i)g_{l\_in,i}, i = 1,\cdots,n \tag{1}$$

$$\bar{r}_{s\_out,i} = 1 - r_{s\_out,i} - g_{s\_out,i}, i = 1,\cdots,n \tag{2}$$

$$r_{l\_out,i} = \bar{\delta}_i g_{s\_in,i}, i = 1,\cdots,n \tag{3}$$

$$\bar{r}_{l\_out,i} = 1 - r_{l\_out,i} - g_{l\_out,i}, i = 1,\cdots,n \tag{4}$$

$$r_{s\_in,i} = (1-\bar{\delta}_i)g_{l\_out,i}, i = 1,\cdots,n \tag{5}$$

$$\bar{r}_{s\_in,i} = 1 - r_{s\_in,i} - g_{s\_in,i}, i = 1,\cdots,n \tag{6}$$

$$r_{l\_in,i} = \delta_i g_{s\_out,i}, i = 1,\cdots,n \tag{7}$$

Figure 1 Illustration of NEMA phase structure

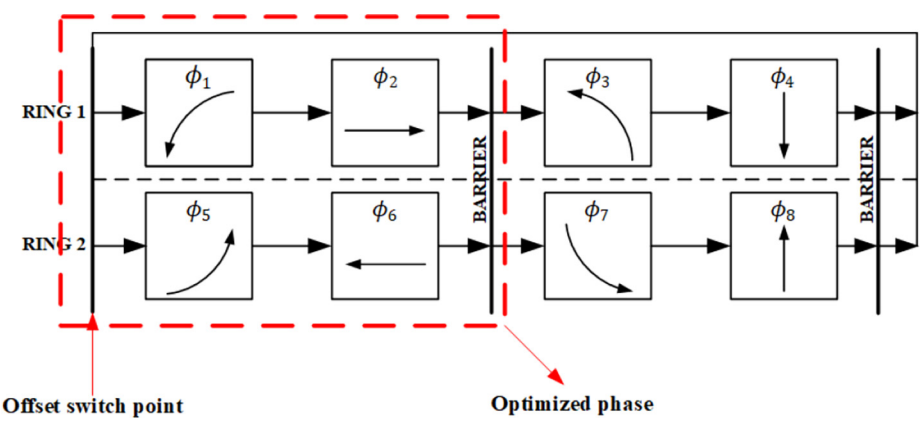

$$\overline{r}_{l\_in,i} = 1 - r_{l\_in,i} - g_{l\_in,i}, i = 1, \cdots, n \tag{8}$$

In equation (1), the red time before the outbound straight-moving phase is calculated based on the value of δ_i. When δ_i is equal to one, it means that there is no other phase before outbound straight-moving phase. Then, $r_{s\_out,i}$ is equal to zero. When δ_i is equal to zero, it means that the inbound left-turning phase is before the outbound straight-moving phase. Then, $r_{s\_out,i}$ is equal to the green time of the inbound left-turning phase. The red time after the outbound straight-moving phase can be obtained by equation (2). Similarly, the red time before/after other three phases can be calculated by equations (3)–(8).

2.3.2 Progression constraints for regular vehicles

In the model, we try to design a progression band for RVs to maintain the efficiency of RVs. The constraints for progression band are listed in equations (9)–(14). The progress of green bands for outbound and inbound directions are presented in Figure 2.

$$\frac{1}{2}b_i \le w_i \le g_{s\_out,i} - \frac{1}{2}b_i, i = 1, \cdots, n-1 \tag{9}$$

$$\frac{1}{2}b_i \le w_{i+1} + \tau_{i+1} \le g_{s\_out,i+1} - \frac{1}{2}b_i, i = 1, \cdots, n-1 \tag{10}$$

$$\frac{1}{2}\overline{b}_i \le \overline{w}_i - \overline{\tau}_i \le g_{s\_in,i} - \frac{1}{2}\overline{b}_i, i = 1, \cdots, n-1 \tag{11}$$

$$\frac{1}{2}\overline{b}_i \le \overline{w}_{i+1} \le g_{s_{in},i+1} - \frac{1}{2}\overline{b}_i, i = 1, \cdots, n-1 \tag{12}$$

$$\theta_i + r_{s_{out},i} + w_i + t_i + n_i = \theta_{i+1} + r_{s_{out},i+1} + w_{i+1} + \tau_{i+1} + n_{i+1}, i = 1, \cdots, n-1 \tag{13}$$

$$-\theta_i + \overline{r}_{s\_in,i} + \overline{w}_i + \overline{t}_i - \overline{\tau}_i + \overline{n}_i = -\theta_{i+1} + \overline{r}_{s\_in,i+1} + \overline{w}_{i+1} + \overline{n}_{i+1}, i = 1, \cdots, n-1 \tag{14}$$

Equations (9) and (10) are used to limit the outbound band within the available green time. And equations (11) and (12) are for inbound band. Equations (13) and (14) represent the progression process of the green band. By applying these equations and objective, two-way progression bands for RVs will be optimized.

2.3.3 Non-stop constraints for connected and autonomous vehicles

For all CAVs, we hope there are possible trajectories to go through intersections without stopping. In other words, the time range that CAVs arrive at the intersection within the speed limit should have overlapping areas with green time. Based on this idea, the non-stop constraints are developed.

First, we defined the time range $\lambda_i(\overline{\lambda}_i)$ that CAVs arrive at intersection i. Equations (15)–(18) give the maximum and minimum travel time along link i in both outbound and inbound directions. The difference between maximum travel time and minimum travel time is the time range, which are conveyed in equations (19) and (20).

$$t_{min,i} = \frac{d_i}{v_{max}}, i = 1, \cdots, n-1 \tag{15}$$

$$t_{max,i} = \frac{d_i}{v_{min}}, i = 1, \cdots, n-1 \tag{16}$$

Figure 2 Time–space diagram for RVs progression

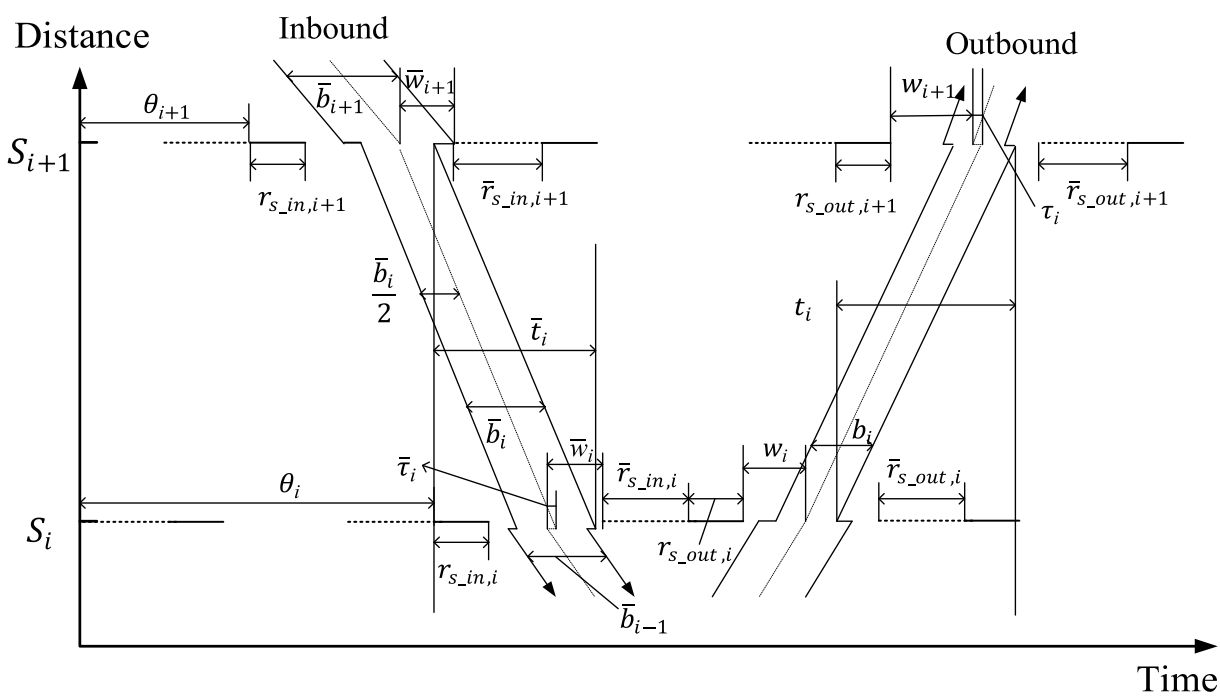

$$\overline{t}_{min,i} = \frac{\overline{d}_i}{v_{max}}, i = 1, \cdots, n-1 \quad (17)$$

$$\overline{t}_{max,i} = \frac{\overline{d}_i}{v_{min}}, i = 1, \cdots, n-1 \quad (18)$$

$$\lambda_{i+1} = t_{max,i} - t_{min,i}, i = 1, \cdots, n-1 \quad (19)$$

$$\overline{\lambda}_i = \overline{t}_{max,i} - \overline{t}_{min,i}, i = 1, \cdots, n-1 \quad (20)$$

Then, the relationship between time range of arrival and green time is analyzed. There are six scenarios in total, which can be seen in Figure 3. Among them, Figure 3(a) shows the scenario that the time range of arrival has no overlapping area with the green time. In Figure 3(b)–(e), all the time ranges of arrival have overlapping area with one part of green time. Furthermore, the time range of arrival has overlapping area with two parts of green time in Figure 3(f). And this scenario can be equal to the scenario in Figure 3(b) or that in Figure 3(e). Several feature points are marked in the Figure. The two sides of time range are represented as **t1** and **t2**, and **g1** and **g2** for those of green time. To find the relationship between overlapping condition and the order of feature points, the values of **t2–g1** and **g2–t1** are analyzed. The results are listed in Table 2. It is demonstrated that all the values of **t2–g1** and **g2–t1** are positive, when time of range has overlapping area with green time. Based on this finding, we can express the overlapping conditions into equations and create nonstop constraints for CAVs.

For RVs, two boundaries can determine a green band. Vehicles can go through the intersection without stopping as long as they travel at a progression speed within the green band. For CAVs, they may enter the intersection at any time of green time. We need to ensure that all these vehicles can go through the upstream intersection without stopping. In other words, their time range of arrival at upstream intersection should have overlapping area with green time. And these CAVs include straight-moving vehicles and left-turning vehicles at upstream intersection. It is more difficult to establish nonstop constraints than band constraints. It is a continuous modeling problem, which should be simplified by discretization method. Through further analysis, we divide the problem into three cases.

Case 1: The time range of arrival is larger than the red time at upstream intersection.

In this case, all CAVs can go through the upstream intersection without stopping. Because the time range of arrival is larger than the red time, the range always has at least one overlapping area with the green time, which can be seen in Figure 4. No constraint is needed in this case.

Case 2: The total time range of all the CAVs' arrival is smaller than the red time at upstream intersection.

In this case, even the total time range of arrival cannot have overlapping area with two parts of green time simultaneously, refer to Figure 5. In other words, all the CAVs entering the current intersection under same green time have to go through the upstream intersection under the same green time. Thus, we just need to make sure that the CAVs entering the current intersection at the start and end of the green time can go through the upstream intersection without stopping. Then, all the CAVs can achieve the nonstop goal. The constraints are established as follows.

Equations (21)–(24) are designed for straight-moving CAVs in the outbound direction. Equations (21) and (22) are used to ensure the CAV entering the current intersection at the start of green time can go straight at upstream intersection without

Figure 3 Relationship between time range of CAVs' arrival and green time

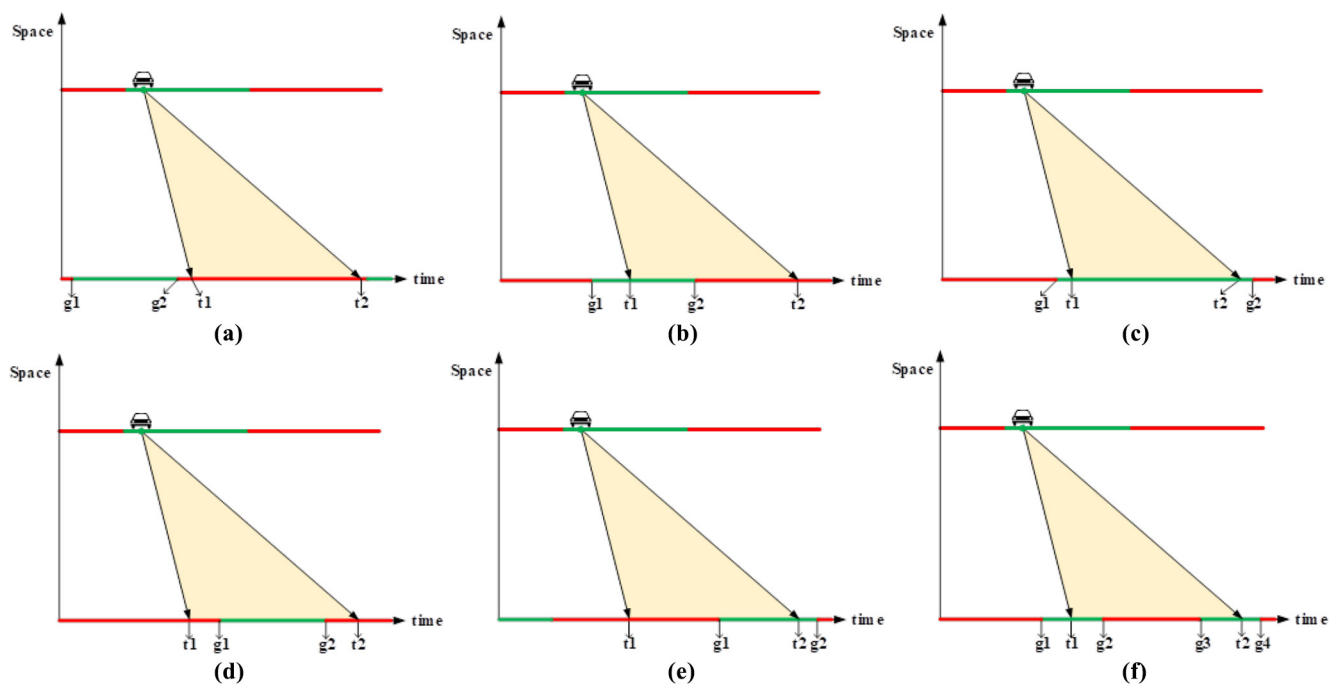

Table 2 Values of **t2-g1** and **g2-t1** under different scenarios

Scenario	t2-g1	g2-t1
(a)	Positive	Negative
(b)	Positive	Positive
(c)	Positive	Positive
(d)	Positive	Positive
(f)	Positive	Positive

stopping. And equations (23) and (24) are for the CAV entering the current intersection at the end of green time:

$$\theta_{i+1} + r_{s\_out,i+1} + g_{s\_out,i+1} + n_{i+1} > \theta_i + r_{s\_out,i} + t_{min,i} + n_i, i = 1, \cdots, n-1 \quad (21)$$

$$\theta_{i+1} + r_{s\_out,i+1} + n_{i+1} < \theta_i + r_{s\_out,i} + t_{max,i} + n_i,$$

Figure 4 Relationship between time range of arrival and signal timing in *Case 1*

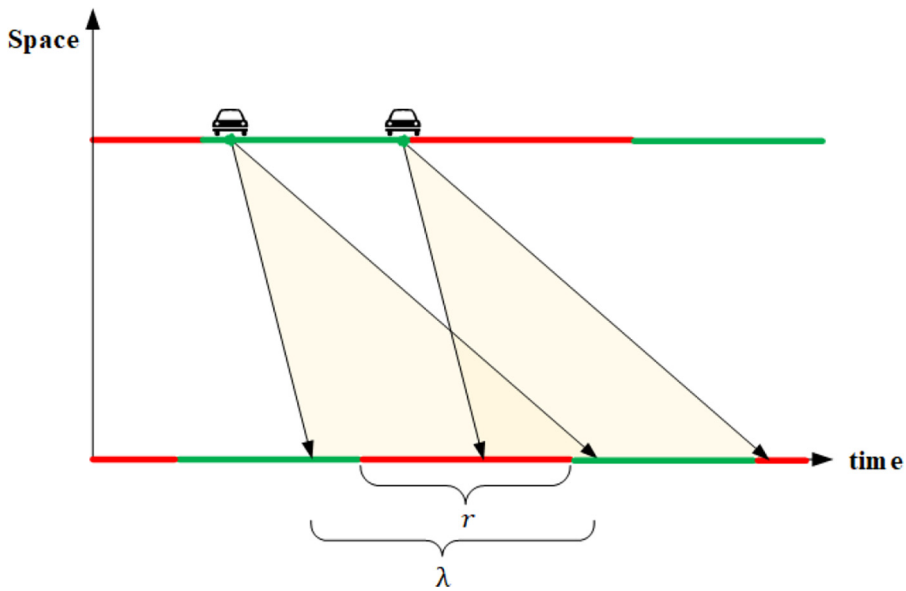

Figure 5 Relationship between time range of arrival and signal timing in *Case 2*

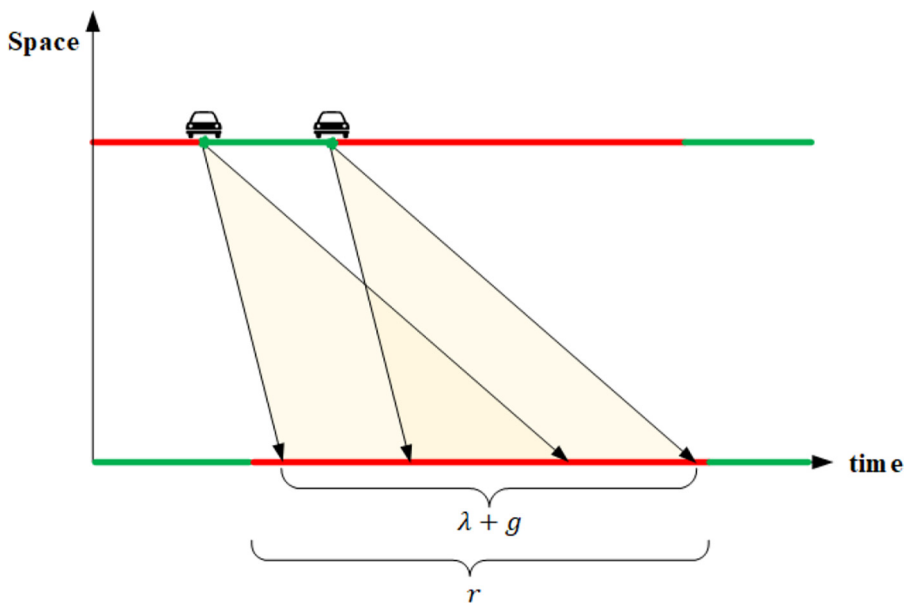

$$i = 1, \cdots, n-1 \tag{22}$$

$$\theta_{i+1} + r_{s\_out,i+1} + g_{s\_out,i+1} + n_{i+1} > \theta_i + r_{s\_out,i} + g_{s\_out,i} + t_{min,i} + n_i, i = 1, \cdots, n-1 \tag{23}$$

$$\theta_{i+1} + r_{s\_out,i+1} + n_{i+1} < \theta_i + r_{s,i} + g_{s\_out,i} + t_{max,i} + n_i, i = 1, \cdots, n-1 \tag{24}$$

Since that,

$$\theta_i + r_{s\_out,i} + g_{s\_out,i} + t_{min,i} + n_i > \theta_i + r_{s\_out,i} + t_{min,i} + n_i, i = 1, \cdots, n-1 \tag{25}$$

$$\theta_i + r_{s\_out,i} + g_{s\_out,i} + t_{max,i} + n_i > \theta_i + r_{s\_out,i} + t_{max,i} + n_i \tag{26}$$

Then, equations (21)–(24) can be simplified to equations (22) and (23).

Similarly, the constraints for left-turning CAVs in the outbound direction are formulated as equations (27) and (28). Equations (29) and (30) are for straight-moving CAVs in the inbound direction. And equations (31) and (32) are for left-turning CAVs in the inbound direction:

$$\theta_{i+1} + r_{l\_out,i+1} + g_{l\_out,i+1} + n_{i+1} > \theta_i + r_{s\_out,i} + g_{s\_out,i} + t_{min,i} + n_i, i = 1, \cdots, n-1 \tag{27}$$

$$\theta_{i+1} + r_{l\_out,i+1} + n_{i+1} < \theta_i + r_{s\_out,i} + t_{max,i} + n_i, \quad i = 1, \cdots, n-1 \tag{28}$$

$$\theta_i - \overline{r}_{s\_in,i} - \overline{n}_i > \theta_{i+1} - \overline{r}_{s\_in,i+1} + \overline{t}_{min,i} - \overline{n}_{i+1}, \quad i = 1, \cdots, n-1 \tag{29}$$

$$\theta_i - \overline{r}_{s\_in,i} - g_{s\_in,i} - \overline{n}_i < \theta_{i+1} - \overline{r}_{s\_in,i+1} - g_{s\_in,i+1} + \overline{t}_{max,i} - \overline{n}_{i+1}, i = 1, \cdots, n-1 \tag{30}$$

$$\theta_i - \overline{r}_{l\_in,i} - \overline{n}_i > \theta_{i+1} - \overline{r}_{s\_in,i+1} + \overline{t}_{min,i} - \overline{n}_{i+1}, \quad i = 1, \cdots, n-1 \tag{31}$$

$$\theta_i - \overline{r}_{l\_in,i} - g_{l\_in,i} - \overline{n}_i < \theta_{i+1} - \overline{r}_{s\_in,i+1} - g_{s\_in,i+1} + \overline{t}_{max,i} - \overline{n}_{i+1}, i = 1, \cdots, n-1 \tag{32}$$

Case 3: The time range of arrival is smaller than the red time at upstream intersection, but the total time range of all the CAVs' arrival is larger than the red time at upstream intersection.

In this case, the total time range of arrival may have overlapping area with one or two parts of green time. If the total time range of arrival has overlapping area with two parts of green time, there will be some moments that CAVs have no possible trajectory to go through the upstream intersection without stopping as shown in Figure 6. Thus, all the CAVs entering the current intersection under same green time have to go through the upstream intersection under the same green time. This conclusion will be proved by discretization method in the following.

The green time will be average divide into m parts to let $\lambda + \frac{q}{m} \leq r$. Then, the subrange of green time will degenerate to *Case 2*. Taking the straight-moving CAVs in outbound direction as an example, equations can be obtained according to conclusion in *Case 2* for the first subrange, which are formulated as follows:

$$\theta_{i+1} + r_{s\_out,i+1} + g_{s\_out,i+1} + n_{i+1} > \theta_i + r_{s\_out,i} + \frac{1}{m} g_{s\_out,i} + t_{min,i} + n_i, i = 1, \cdots, n-1 \tag{33}$$

$$\theta_{i+1} + r_{s\_out,i+1} + n_{i+1} < \theta_i + r_{s\_out,i} + t_{max,i} + n_i, \quad i = 1, \cdots, n-1 \tag{34}$$

For the second subrange, we hold that:

$$\theta_{i+1} + r_{s\_out,i+1} + g_{s\_out,i+1} + n_{i+1} > \theta_i + r_{s\_out,i} + \frac{2}{m} g_{s\_out,i} + t_{min,i} + n_i, i = 1, \cdots, n-1 \tag{35}$$

$$\theta_{i+1} + r_{s\_out,i+1} + n_{i+1} < \theta_i + r_{s\_out,i} + \frac{1}{m} g_{s\_out,i} + t_{max,i} + n_i, i = 1, \cdots, n-1 \tag{36}$$

For the last subrange, equations are as follows:

$$\theta_{i+1} + r_{s\_out,i+1} + g_{s\_out,i+1} + n_{i+1} > \theta_i + r_{s\_out,i} + g_{s\_out,i} + t_{min,i} + n_i, i = 1, \cdots, n-1 \tag{37}$$

$$\theta_{i+1} + r_{s\_out,i+1} + n_{i+1} < \theta_i + r_{s\_out,i} + \frac{m-1}{m} g_{s\_out,i} + t_{max,i} + n_i, i = 1, \cdots, n-1 \tag{38}$$

To summarize and simplify these equations, the constraints for the straight-moving CAVs in outbound direction can be obtained, which are presented in equations (39) and (40).

Figure 6 Relationship between time range of arrival and signal timing in *Case 3*

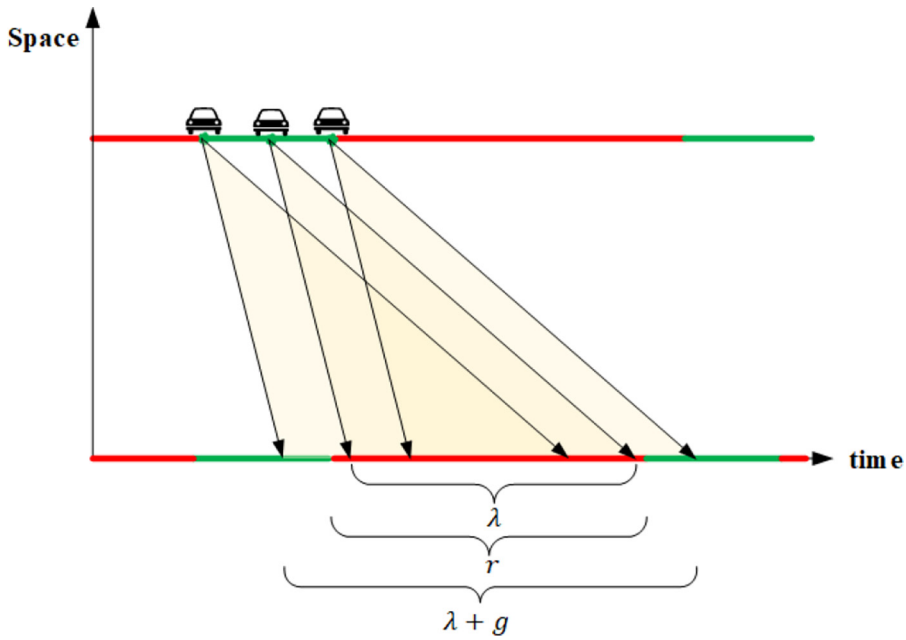

$$\theta_{i+1} + r_{s\_out,i+1} + n_{i+1} < \theta_i + r_{s\_out,i} + t_{max,i} + n_i,$$

$$i = 1, \cdots, n-1 \tag{39}$$

$$\theta_{i+1} + r_{s\_out,i+1} + g_{s\_out,i+1} + n_{i+1} > \theta_i + r_{s\_out,i}$$

$$+ g_{s\_out,i} + t_{min,i} + n_i, i = 1, \cdots, n-1 \tag{40}$$

We can see that these constraints are the same as those in *Case 2*. It demonstrates the finding above that all the CAVs entering the current intersection under same green time have to go through the upstream intersection under the same green time. Then, we can also use the constraints in *Case 2* for other three type of CAVs on the arteries, including left-turning CAVs in outbound direction, straight-moving CAVs in inbound direction and left-turning CAVs in inbound direction.

2.3.4 Objective

$$Max \quad B = \frac{1}{n-1}\sum_{i=1}^{n-1}\left(a_i b_i + \overline{a}_i \overline{b}_i\right) \tag{41}$$

where:

$$a_i = \left(\frac{V_i}{S_i}\right)^p, \overline{a}_i = \left(\frac{\overline{V}_i}{\overline{S}_i}\right)^p \tag{42}$$

And

$V_i(\overline{V}_i)$ = outbound (inbound) total directional volume on link i;
$S_i(\overline{S}_i)$ = outbound (inbound) saturation flow on link i; and
p = exponential power.

3. Case study

3.1 Description of simulated scenario

As there is no dedicated CAV lane in real world, an artery consisting of eight intersections is designed for simulation. The length of artery is 4.0 km. Both outbound and inbound directions have one dedicated CAV lane. Straight-moving CAVs and left-turning CAVs can all be driven on the dedicated lane. In addition, CAVs can overtake via regular lanes, but RVs are not allowed to enter the dedicated CAV lane.

To verify the efficiency of the proposed method, two different volume scenarios were designed. One is a high-volume scenario, the other is a medium-volume scenario. For low-volume scenario, cycle length will be small. All CAVs have potential trajectories to pass intersections without stopping. Thus, low-volume scenario was not considered in this paper. The input RV flowrates of two scenarios are presented in Table 3. The timing plans were first calculated according to the procedure in Highway Capacity Manual (HCM). Then the largest cycle length was selected as the common cycle length. The common cycle lengths were 149 s and 90 s for high-volume scenario and medium-volume scenario, respectively. MULTIBAND and the modified model in this paper were used to optimize offsets and phase sequences. For CAVs, the effects of flowrate and left-turning proportion were tested. The minimum of input flowrate was 60 veh/h. Then, the flowrate was increased to 60 veh/h every time until the flowrate reached 480 veh/h. Left-turning proportion was tested by four different inputs, including 0%, 5%, 10% and 15%. To combine these two factors, there were 32 different combinations designed for each scenario.

A simple control strategy was proposed to take the advantages of CAV, which allows CAVs to go through intersections without stopping. The process of control strategy is demonstrated in Figure 7. When a CAV goes through the current intersection, it can obtain the distance to the

Table 3 Input flowrate of RV

(a) High-volume scenario

		East bound (pcu/h)			West bound (pcu/h)			South bound (pcu/h)			North bound (pcu/h)		
No.	**Distance (m)**	**LT**	**TH**	**RT**	**LT**	**TH**	**RT**	**LT**	**TH**	**RT**	**LT**	**TH**	**RT**
1	-	387	826	124	254	699	56	428	451	43	328	434	62
2	417	378	866	72	392	723	12	284	362	21	265	319	35
3	493	334	799	42	294	802	68	309	457	26	299	413	12
4	700	249	814	57	254	886	70	302	460	12	266	368	40
5	588	436	698	22	378	765	128	489	759	188	257	719	102
6	435	294	965	30	278	1,044	22	148	112	4	223	100	10
7	629	287	816	10	291	1032	33	562	470	78	234	453	54
8	691	264	1,148	20	208	832	52	214	400	12	512	210	100

(b) Medium-volume scenario

No.	Distance (m)	East bound (pcu/h)			West bound (pcu/h)			South bound (pcu/h)			North bound (pcu/h)		
		LT	TH	RT	LT	TH	RT	LT	TH	RT	LT	TH	RT
1	–	329	702	105	216	594	48	364	383	37	279	369	53
2	417	321	736	61	333	615	10	241	308	18	225	271	30
3	493	284	679	36	250	682	58	263	388	22	254	351	10
4	700	212	692	48	216	753	60	257	391	10	226	313	34
5	588	371	593	19	321	650	109	416	645	160	218	611	87
6	435	250	820	26	236	887	19	126	95.2	3.4	190	85	8.5
7	629	244	694	8.5	247	877	28	478	400	66	199	385	46
8	691	224	976	17	177	707	44	182	340	10	435	179	85

Figure 7 Control strategy for CAVs to pass intersection without stopping

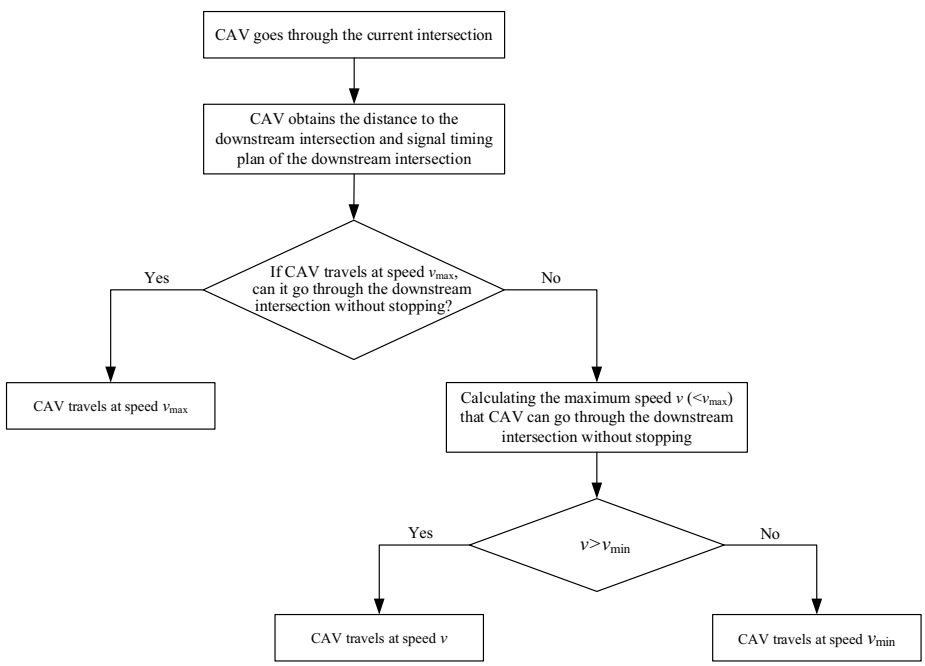

downstream intersection and the signal timing plan of the downstream intersection. Then, it is determined whether the CAV can go through the downstream intersection without stopping when traveling at speed v_{max}. If it can go through the downstream intersection without stopping at speed v_{max}, the CAV will travel at average speed v_{max}. Because v_{max} is the maximum average speed, CAVs cannot exceed this speed. And CAVs can also pass the downstream intersection without stopping at this speed. Otherwise, another largest possible speed v, which is smaller than maximum speed, will be calculated to guarantee that the CAV can go through the downstream without stop. A comparison will be made between the calculated speed v and CAV's minimum average speed v_{min}. If v is larger than v_{min}, the CAV will travel at average speed v. The reason is that if CAVs travel at a speed larger than v, they will stop at the downstream intersection. Though total travel time is almost

Table 4 Average speed improvement of the modified model compared to MULTIBAND for high-volume scenario

		Left-turning proportion of CAV							
		0		5%		10%		15%	
Flowrate of CAV (veh/h)		Average speed (km/h)	Improvement	Average speed (km/h)	Improvement	Average speed (km/h)	Improvement	Average speed (km/h)	Improvement
60	M-B	36.51	6.22%	33.52	18.45%	32.88	20.12%	31.37	26.14%
	M	38.78		39.70		39.49		39.57	
120	M-B	35.63	8.32%	33.77	15.84%	32.48	17.50%	31.37	18.90%
	M	38.59		39.12		38.16		37.30	
180	M-B	35.59	7.00%	34.07	13.10%	32.39	16.99%	31.45	17.42%
	M	38.08		38.53		37.89		36.93	
240	M-B	35.42	6.33%	33.69	12.95%	32.27	15.03%	31.11	18.71%
	M	37.66		38.05		37.12		36.94	
300	M-B	35.33	6.20%	32.66	14.46%	31.54	17.84%	31.26	16.29%
	M	37.52		37.38		37.16		36.36	
360	M-B	35.51	4.81%	33.40	11.80%	31.55	17.73%	30.53	19.30%
	M	37.21		37.34		37.14		36.42	
420	M-B	35.57	4.98%	31.49	17.23%	32.05	15.46%	29.97	21.11%
	M	37.34		36.91		37.00		36.30	
480	M-B	35.50	5.30%	33.46	8.92%	31.87	13.13%	29.55	22.38%
	M	37.38		36.45		36.05		36.16	

Note: M-B represents MULTIBAND model, M represents modified model

Table 5 Average delay improvement of the modified model compared to MULTIBAND for high-volume scenario

		Left-turning proportion of CAV							
		0		5%		10%		15%	
Flowrate of CAV (veh/h)		Average delay (s/veh)	Improvement	Average delay (s/veh)	Improvement	Average delay (s/veh)	Improvement	Average delay (s/veh)	Improvement
60	M-B	169.66	10.08%	141.86	26.86%	119.63	30.54%	121.66	35.66%
	M	152.56		103.76		83.10		78.27	
120	M-B	173.09	11.30%	140.2	23.15%	129.45	25.01%	122.88	25.78%
	M	153.53		107.74		97.08		91.20	
180	M-B	178.66	9.56%	148.98	19.24%	135.37	23.00%	128.43	24.46%
	M	161.58		120.32		104.24		97.01	
240	M-B	184.55	9.27%	153.39	18.33%	139.99	20.83%	129.56	26.50%
	M	167.45		125.27		110.83		95.23	
300	M-B	186.67	8.57%	164.32	20.04%	146.28	23.65%	133.08	22.91%
	M	170.68		131.39		111.69		102.59	
360	M-B	189.43	7.03%	160.16	16.55%	146.55	24.27%	135.07	25.96%
	M	176.12		133.66		110.98		100.00	
420	M-B	188.6	7.24%	180.23	23.02%	147.41	21.37%	137.77	27.68%
	M	174.94		138.74		115.91		99.63	
480	M-B	191.62	8.08%	162.63	12.99%	149.51	18.84%	139.47	28.31%
	M	176.13		141.51		121.34		99.98	

Table 6 Comparison of RV performance between MULTIBAND and the modified model for high-volume scenario

Model	Average delay (s/veh)	Average speed (km/h)	Average stops
MULTIBAND	164.80	26.51	4.93
Modified model	167.28	26.34	5.24

the same, the restarting of CAVs will consume more energy. If v is larger than v_{min}, the CAV will travel at average speed v_{min}.

In the modeling process, it is assumed that there is no significant interference between CAVs and RVs. More sophisticated control strategies are needed to achieve the results, which cannot be realized in current commercial traffic simulation program. To obtain the operation results of RVs and CAVs, the two types of vehicles are simulated separately in a

same road network. For high-volume scenario, the progression speed of RVs is set as 40 km/h. And the speed range of CAVs is set from 28 to 80 km/h. For medium-volume scenario, the progression speed of RVs is set as 60 km/h. And the speed range of CAVs is set from 28 to 100 km/h. Thus, the method in this paper can be tested with different progression speeds. The simulation is conducted by SUMO traffic simulation program, in which CAVs can be controlled according to the designed strategy. A comparison is conducted between MULTIBAND and the modified model in this paper.

3.2 Comparisons and evaluations

The efficiency of both two types of vehicles is obtained to evaluate the performance of two models in terms of average speed and average delay. The average speed can be obtained as total distance over total travel time. The comparison results are presented in Tables 4–6 and Figure 8. The average delay is calculated as follows:

$$\text{Delay} = \frac{1}{N}\sum_{i=1}^{N}\left(T_i - \frac{D_i}{v_{max}}\right) \tag{43}$$

where N is the total number of vehicles, T_i is the travel time of vehicle i and D_i is the travel distance of vehicle i.

The performance improvement is also calculated to evaluate the two models. The improvement is calculated by equations (44) and (45):

$$\text{SI} = \frac{V_{\text{M}} - V_{\text{M-B}}}{V_{\text{M-B}}} \times 100\% \tag{44}$$

$$\text{DI} = \frac{de_{\text{M-B}} - de_{\text{M}}}{de_{\text{M-B}}} \times 100\% \tag{45}$$

where SI is the average speed improvement, DI is the average delay improvement, V_{M} is the average speed of CAVs for modified model, $V_{\text{M-B}}$ is the average speed of CAVs for MULTIBAND, de_{M} is the average delay of CAVs for modified model and $de_{\text{M-B}}$ is the average delay of CAVs for MULTIBAND.

3.2.1 High-volume scenario

The results for high-volume scenario are presented in Tables 4–6 and Figure 8.

Figure 8 CAV performance comparison between MULTIBAND and the modified model for high-volume scenario

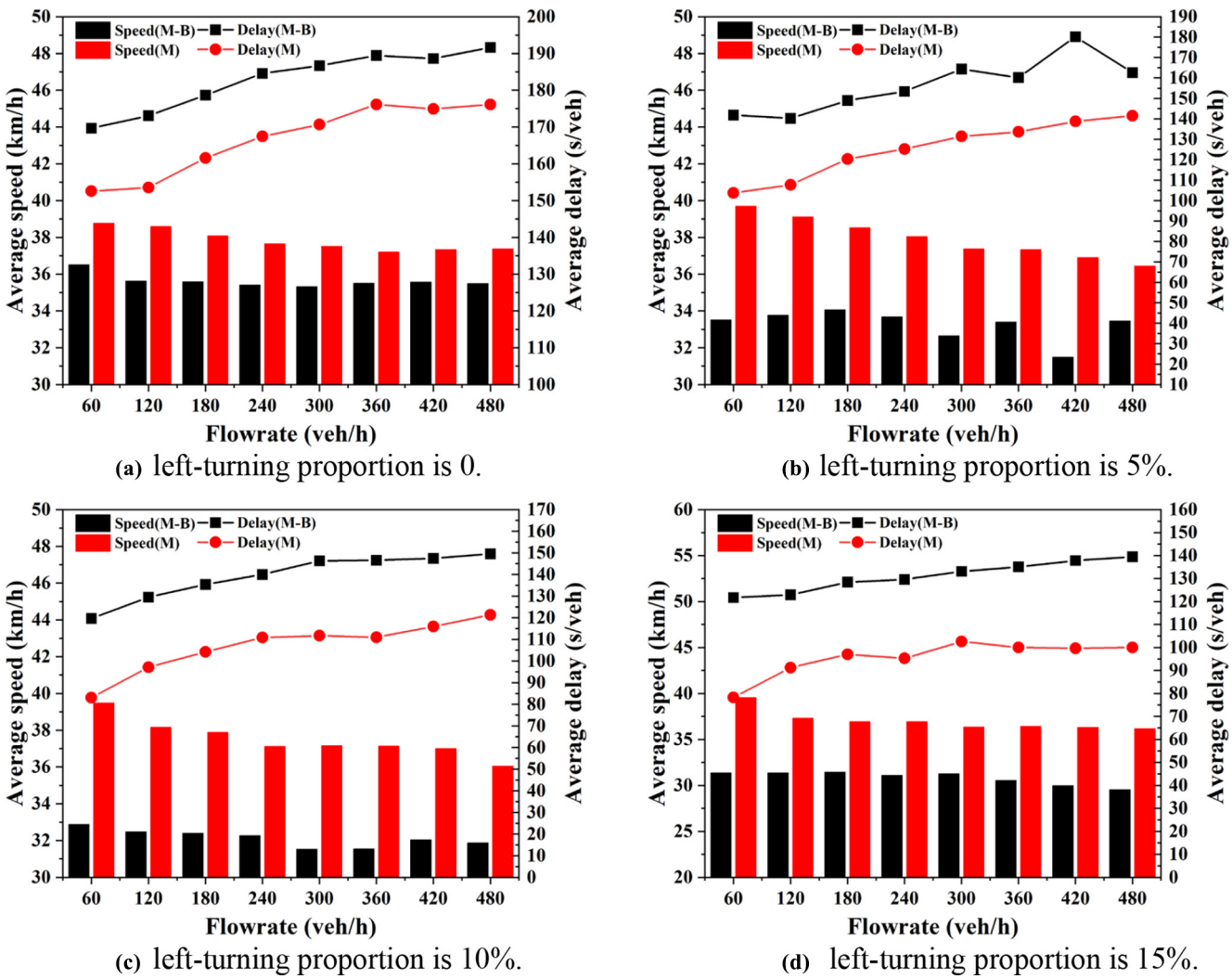

(a) left-turning proportion is 0.

(b) left-turning proportion is 5%.

(c) left-turning proportion is 10%.

(d) left-turning proportion is 15%.

At first, it can be seen that CAVs travel much faster than RVs with two signal timing plans, which proves that CAVs have significant advantage over RVs in terms of travel efficiency. Then, we compared the performance of two models. In Figure 8, it is obvious that modified model outperformed MULTIBAND model in all scenarios. In other words, CAVs can play to their strengths better with the signal timing plan generated by modified model. In terms of average speed, the maximum improvement can be 24.20%, which can be found in Table 4. As for average delay, the maximum improvement can be 32.20%, which can be found in Table 5. Further, we analyzed the effect of flowrate and left-turning proportion of CAVs. With the increase of CAV flowrate, the average speed for two models decreases. Meanwhile, the average delay for two models increases. The improvement first decreases and then increases. With the increase of left-turning proportion, the improvement becomes larger. Furthermore, with higher left-turning proportion, the average delay and average speed for MULTIBAND are more affected than those for modified model. It is because the CAV's characteristics are not

Table 7 Average speed improvement of the modified model compared to MULTIBAND for medium-volume scenario

		Left-turning proportion of CAV							
		0		5%		10%		15%	
Flowrate of CAV (veh/h)		Average speed (km/h)	Improvement	Average speed (km/h)	Improvement	Average speed (km/h)	Improvement	Average speed (km/h)	Improvement
60	M-B	50.44	12.16%	49.32	7.40%	48.78	7.19%	46.85	7.58%
	M	56.58		52.97		52.29		50.41	
120	M-B	51.25	5.52%	49.18	9.69%	47.05	9.54%	47.55	4.49%
	M	54.08		53.94		51.54		49.68	
180	M-B	51.23	6.65%	49.42	5.55%	47.50	8.20%	44.84	11.50%
	M	54.64		52.16		51.40		50.00	
240	M-B	51.83	4.68%	49.01	7.32%	46.49	9.37%	46.23	5.16%
	M	54.26		52.60		50.85		48.62	
300	M-B	51.61	4.68%	49.05	7.24%	47.19	7.04%	45.70	7.10%
	M	54.02		52.60		50.52		48.94	
360	M-B	51.45	4.65%	49.30	5.84%	46.26	8.37%	45.72	6.09%
	M	53.85		52.18		50.13		48.51	
420	M-B	51.33	4.20%	48.43	7.44%	47.16	6.47%	43.44	9.30%
	M	53.48		52.04		50.21		47.48	
480	M-B	51.30	4.67%	48.48	6.57%	46.68	6.31%	44.35	6.91%
	M	53.70		51.67		49.63		47.42	

Table 8 Average delay improvement of the modified model compared to MULTIBAND for medium-volume scenario

		Left-turning proportion of CAV							
		0		5%		10%		15%	
Flowrate of CAV (veh/h)		Average delay (s/veh)	Improvement	Average delay (s/veh)	Improvement	Average delay (s/veh)	Improvement	Average delay (s/veh)	Improvement
60	M-B	136.64	15.37%	100.55	11.98%	84.01	11.49%	82.96	12.38%
	M	115.64		88.50		74.36		72.69	
120	M-B	133.83	7.10%	102.85	13.55%	95.66	13.23%	82.68	7.41%
	M	124.33		88.91		83.00		76.55	
180	M-B	138.34	9.77%	110.97	8.08%	97.86	11.44%	95.43	15.75%
	M	124.82		102.00		86.66		80.40	
240	M-B	139.56	7.05%	114.71	10.86%	104.69	12.48%	89.65	7.82%
	M	129.72		102.25		91.62		82.64	
300	M-B	141.23	7.19%	116.80	10.98%	102.26	9.97%	95.05	10.49%
	M	131.07		103.98		92.06		85.08	
360	M-B	144.18	7.50%	117.82	9.09%	105.41	12.29%	93.07	8.82%
	M	133.37		107.11		92.45		84.86	
420	M-B	143.93	6.80%	122.74	10.83%	105.66	9.27%	99.94	12.52%
	M	134.14		109.45		95.87		87.43	
480	M-B	145.26	6.65%	122.10	9.76%	108.47	9.70%	96.40	9.81%
	M	135.60		110.18		97.95		86.94	

considered in the MULTIBAND modeling. When flowrate of CAVs becomes larger with higher left-turning proportion, the efficiency of straight-moving CAVs will be affected by left-turning CAVs significantly.

Table 6 gives RV progression efficiency results with two models. The efficiency of RVs is not affected significantly.

3.2.2 Medium-volume scenario

The results for medium-volume scenario are presented in Tables 7–9 and Figure 9.

The modified model in this paper can still improve the CAV efficiency under medium-volume scenario with high progression speed. Similar trends can be found from the results. With the increase of CAV flowrate, the average speed decreases, and the average delay decreases, which can be found in both models. With the increase of left-turning proportion, average speed decreases. It is because CAVs from side streets were not considered in the optimization. A substantial proportion of CAVs have to wait at intersections. The average speed of CAVs is affected. Compared to high-volume scenario, the improvement becomes smaller. It is indicated that the modified model is effective with different progression speeds but performs better with lower progression speed.

From the comparison of performance above, it can be concluded that just laying out a dedicated CAV lane will not give full play to the advantages of CAVs. With traditional arterial signal coordination plan, the superiority of dedicated CAV lane is not significant. Though trajectories of CAVs can be optimized, the Signal timing scheme is the basis of optimization. A signal optimization without consideration of the characteristics of CAVs limits the optimization, especially with high CAV flowrate. Under this situation, there are two choices for CAVs. One is to travel at a high speed and stop at

Table 9 Comparison of RV performance between MULTIBAND and the modified model for medium-volume scenario

Model	Average delay (s/veh)	Average speed (km/h)	Average stops
MULTIBAND	121.83	40.89	2.36
Modified model	103.74	44.51	2.83

Figure 9 CAV performance comparison between MULTIBAND and the modified model for medium-volume scenario

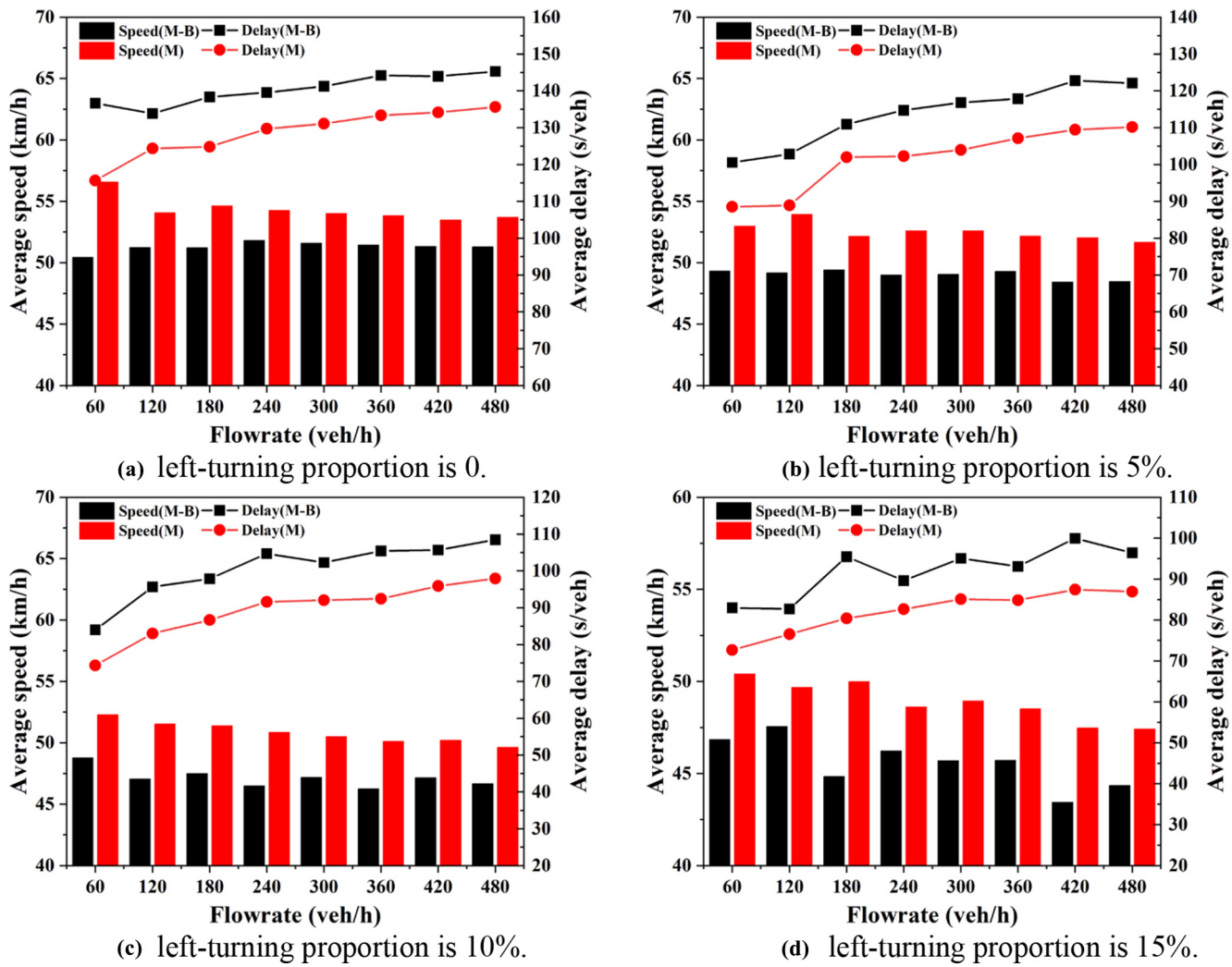

Figure 10 CAV performance with different minimum speed limitations

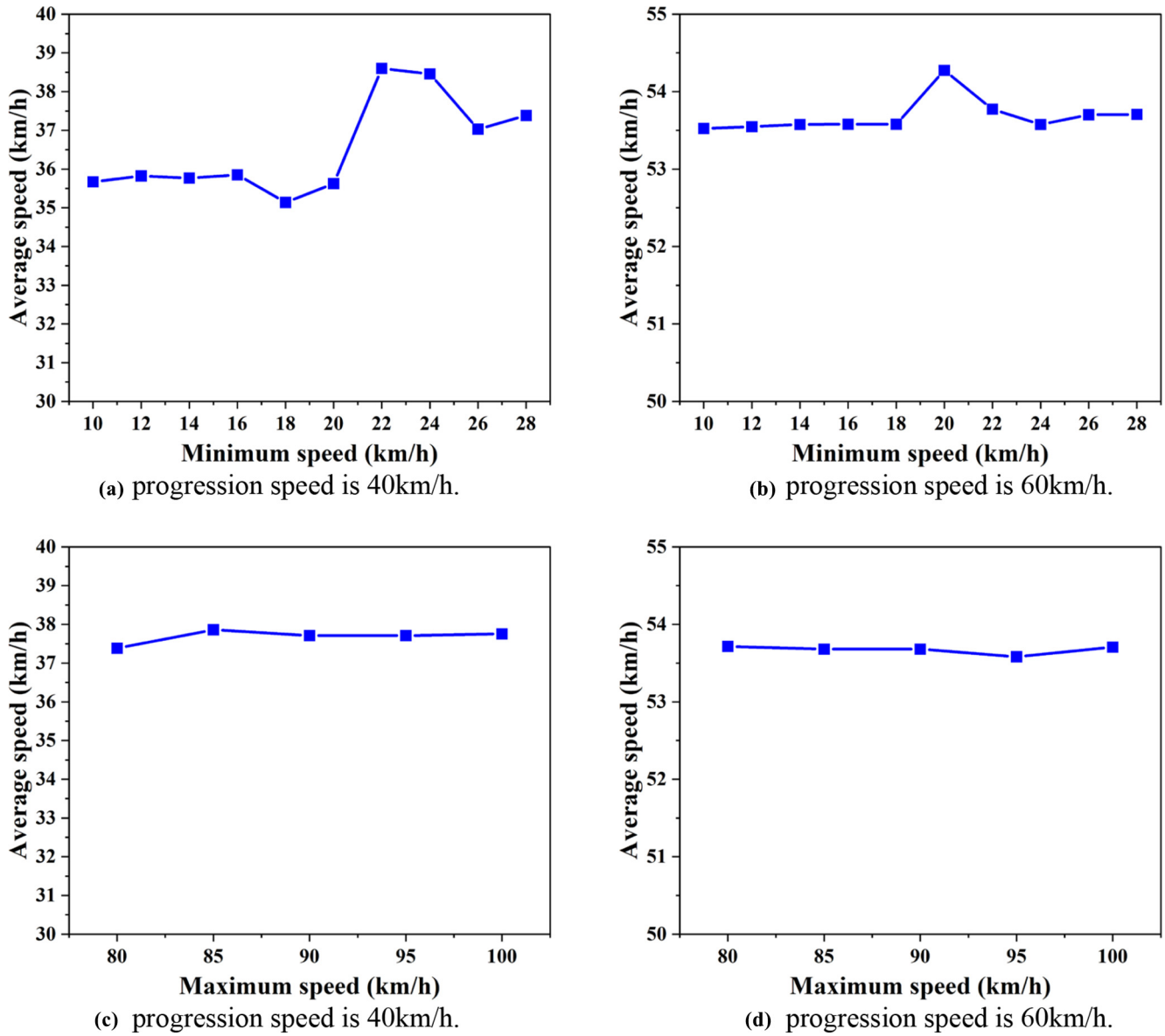

intersections, then wait for a long time. The other is to travel at a very low speed to avoid stopping. These two operations will both affect the efficiency of CAVs. If signal coordination plan can be optimized with CAV's characteristics, a corridor can be established for CAVs. CAVs can travel at a higher speed than RVs without stopping.

4. Sensitivity analysis

In the modeling process, speed limitation of a CAV is introduced in the model. The effect of speed limitation is analyzed in this subsection, which includes minimum speed and maximum speed. The results are presented in Figure 10. The CAV flowrate is set as 480 veh/h. The turning proportion is set as 0.

The modified model is infeasible when minimum speed is larger than 28 km/h and maximum speed is smaller than 80 km/h for both two scenarios. It is indicated that the boundary of speed limitation is not decided by the progression speed. Instead, it is decided by the distance between intersections.

Ten different minimum speeds were tested to evaluate the effect of minimum speed, which is from 10 to 28 km/h. When the progression speed is 40 km/h, it can be seen that the CAV can achieve higher efficiency with higher minimum speed. With the decrease of minimum speed, the average speed of the CAV is almost the same. When the progression speed is 60 km/h, the CAV efficiency is not affected significantly. Because speed difference from 28 to 60 km/h is larger than that from 28 to 40 km/h. Only in a certain range of speed, the decrease of minimum speed will affect the CAV efficiency.

Five different maximum speeds were analyzed, including 80, 85, 90, 95 and 100 km/h. It is obvious that the CAV efficiency is not affected by the value of maximum speed significantly in two scenarios. It indicates that a CAV can achieve the proposed control strategy with 80 km/h under two scenarios.

5. Conclusion

CAVs have remarkable advantages over RVs in many aspects. CAVs can communicate with other traffic participants and can do all the driving in all circumstances by themselves. However, full-scale benefits of CAVs can only be achieved at 100% CAV penetration. In a period of transition, dedicated CAV lanes are preferable to attain the positive effects of CAVs. In this research, a signal coordination model for arteries with dedicated CAV lanes is proposed to enhance the CAV efficiency under mixed traffic flow. Different from RVs, non-stop behavior is treated as the constraints for CAVs, which was established with continuous modeling method. To verify the efficiency, the proposed model was compared to MULTIBAND under high-volume scenario and medium-volume scenario. The results indicated that CAV efficiency can be improved significantly with the timing plan generated by the proposed model. It is vital to consider the characteristics of CAV when optimizing the arterial signal with dedicated CAV lanes.

Significant improvement in CAV efficiency was achieved in this paper. However, there are still many aspects that can be modified. Only a crude CAV speed control strategy was proposed in this paper, which needs further improvement to achieve eco-driving. The objective of the model was not associated with CAV's efficiency, which leads to the limitation of improvement.

References

Arsava, T., Xie, Y. and Gartner, N.H. (2016), "Arterial progression optimization using OD-BAND: case study and extensions", *Transportation Research Record: Journal of the Transportation Research Board*, Vol. 2558 No. 1, pp. 1-10.

Arvin, R., Khattak, A.J., Kamrani, M. and Rio-Torres, J. (2021), "Safety evaluation of connected and automated vehicles in mixed traffic with conventional vehicles at intersections", *Journal of Intelligent Transportation Systems*, Vol. 25 No. 2, pp. 170-187.

Beak, B., Head, K.L. and Feng, Y. (2017), "Adaptive coordination based on connected vehicle technology", *Transportation Research Record: Journal of the Transportation Research Board*, Vol. 2619 No. 1, pp. 1-12.

Carrone, A.P., Rich, J., Vandet, C.A. and An, K. (2021), "Autonomous vehicles in mixed motorway traffic: capacity utilisation, impact and policy implications", *Transportation*, Vol. 48 No. 6, pp. 1-32.

Chang, X., Li, H., Rong, J. and Zhao, X. (2020), "Analysis on traffic stability and capacity for mixed traffic flow with platoons of intelligent connected vehicles", *Physica A: Statistical Mechanics and Its Applications*, Vol. 557, p. 124829.

Du, Y., ShangGuan, W. and Chai, L. (2021), "A coupled vehicle-signal control method at signalized intersections in mixed traffic environment", *IEEE Transactions on Vehicular Technology*, Vol. 70 No. 3, pp. 2089-2100.

Fayazi, S.A. and Vahidi, A. (2018), "Mixed-integer linear programming for optimal scheduling of autonomous vehicle intersection crossing", *IEEE Transactions on Intelligent Vehicles*, Vol. 3 No. 3, pp. 287-299.

Feng, Y., Yu, C. and Liu, H.X. (2018), "Spatiotemporal intersection control in a connected and automated vehicle environment", *Transportation Research Part C: Emerging Technologies*, Vol. 89, pp. 364-383.

Gartner, N.H., Assmann, S.F., Lasaga, F.L. and Hou, D.L. (1991), "A multi-band approach to arterial traffic signal optimization", *Transportation Research Part B: Methodological*, Vol. 25 No. 1, pp. 55-74.

Ghiasi, A., Hussain, O., Qian, Z.S. and Li, X. (2017), "A mixed traffic capacity analysis and lane management model for connected automated vehicles: a Markov chain method", *Transportation Research Part B: Methodological*, Vol. 106, pp. 266-292.

Goodall, N.J., Smith, B.L. and Park, B. (2013), "Traffic signal control with connected vehicles", *Transportation Research Record: Journal of the Transportation Research Board*, Vol. 2381 No. 1, pp. 65-72.

Guo, Q., Li, L. and Ban, X.J. (2019a), "Urban traffic signal control with connected and automated vehicles: a survey", *Transportation Research Part C: emerging Technologies*, Vol. 101, pp. 313-334.

Guo, Y., Ma, J., Xiong, C., Li, X., Zhou, F. and Hao, W. (2019b), "Joint optimization of vehicle trajectories and intersection controllers with connected automated vehicles: combined dynamic programming and shooting heuristic approach", *Transportation Research Part C: emerging Technologies*, Vol. 98, pp. 54-72.

He, X., Liu, H.X. and Liu, X. (2015), "Optimal vehicle speed trajectory on a signalized arterial with consideration of queue", *Transportation Research Part C: Emerging Technologies*, Vol. 61, pp. 106-120.

Hu, G., Lu, W., Whalin, R.W., Wang, F. and Kwembe, T.A. (2021), "Analytical approximation for macroscopic fundamental diagram of urban corridor with mixed human and connected and autonomous traffic", *IET Intelligent Transport Systems*, Vol. 15 No. 2, pp. 261-272.

Larsson, J., Keskin, M.F., Peng, B., Kulcsár, B. and Wymeersch, H. (2021), "Pro-social control of connected automated vehicles in mixed-autonomy multi-lane highway traffic", *Communications in Transportation Research*, Vol. 1, p. 100019.

Li, Z., Elefteriadou, L. and Ranka, S. (2014), "Signal control optimization for automated vehicles at isolated signalized intersections", *Transportation Research Part C: Emerging Technologies*, Vol. 49, pp. 1-18.

Litman, T. (2017), *Autonomous Vehicle Implementation Predictions*, Victoria Transport Policy, Victoria.

Little, J.D., Kelson, M.D. and Gartner, N.H. (1981), "MAXBAND: a program for setting signals on arterials and triangular networks", *Transportation Research Record*, Vol. 759, pp. 40-46.

Ma, W., Zou, L., An, K., Gartner, N.H. and Wang, M. (2018), "A partition-enabled multi-mode band approach to arterial traffic signal optimization", *IEEE Transactions on Intelligent Transportation Systems*, Vol. 20 No. 1, pp. 313-322.

Peng, B., Keskin, M.F., Kulcsár, B. and Wymeersch, H. (2021), "Connected autonomous vehicles for improving mixed traffic efficiency in unsignalized intersections with deep reinforcement learning", *Communications in Transportation Research*, Vol. 1, p. 100017.

Qian, G., Guo, M., Zhang, L., Wang, Y., Hu, S. and Wang, D. (2021), "Traffic scheduling and control in fully connected

and automated networks", *Transportation Research Part C: Emerging Technologies*, Vol. 126, p. 103011.

Sala, M. and Soriguera, F. (2021), "Capacity of a freeway lane with platoons of autonomous vehicles mixed with regular traffic", *Transportation Research Part B: Methodological*, Vol. 147, pp. 116-131.

Shi, X., Wang, Z., Li, X. and Pei, M. (2021), "The effect of ride experience on changing opinions toward autonomous vehicle safety", *Communications in Transportation Research*, Vol. 1, p. 100003.

Sinha, A., Chand, S., Wijayaratna, K.P., Virdi, N. and Dixit, V. (2021), "Comprehensive safety assessment in mixed fleets with connected and automated vehicles: a crash severity and rate evaluation of conventional vehicles", *Accident Analysis & Prevention*, Vol. 142, p. 105567.

Xu, B., Ban, X.J., Bian, Y., Li, W., Wang, J., Li, S.E. and Li, K. (2018), "Cooperative method of traffic signal optimization and speed control of connected vehicles at isolated intersections", *IEEE Transactions on Intelligent Transportation Systems*, Vol. 20 No. 4, pp. 1390-1403.

Yang, Z., Feng, Y. and Liu, H.X. (2021), "A cooperative driving framework for urban arterials in mixed traffic conditions", *Transportation Research Part C: emerging Technologies*, Vol. 124, p. 102918.

Zeng, X., Sun, X., Zhang, Y. and Quadrifoglio, L. (2015), "Person-based adaptive priority signal control with connected-vehicle information", *Transportation Research Record: Journal of the Transportation Research Board*, Vol. 2487 No. 1, pp. 78-87.

Zhang, C., Xie, Y., Gartner, N.H., Stamatiadis, C. and Arsava, T. (2015), "AM-band: an asymmetrical multi-band model for arterial traffic signal coordination", *Transportation Research Part C: Emerging Technologies*, Vol. 58, pp. 515-531.

Zhang, L., Song, Z., Tang, X. and Wang, D. (2016), "Signal coordination models for long arterials and grid networks", *Transportation Research Part C: Emerging Technologies*, Vol. 71, pp. 215-230.

Further reading

Niroumand, R., Tajalli, M., Hajibabai, L. and Hajbabaie, A. (2020), "Joint optimization of vehicle-group trajectory and signal timing: introducing the white phase for mixed-autonomy traffic stream", *Transportation Research Part C: emerging Technologies*, Vol. 116, p. 102659.

Yu, C., Feng, Y., Liu, H.X., Ma, W. and Yang, X. (2018), "Integrated optimization of traffic signals and vehicle trajectories at isolated urban intersections", *Transportation Research Part B: Methodological*, Vol. 112, pp. 89-112.

Corresponding author

Sheng Jin can be contacted at: jinsheng@zju.edu.cn